UC San Diego
UC San Diego Previously Published Works

Title
Asymmetry in the Seasonal Cycle of Zonal-Mean Surface Air Temperature

Permalink
https://escholarship.org/uc/item/0d38r0jx

Journal
Geophysical Research Letters, 50(10)

ISSN
0094-8276

Authors
Roach, Lettie A
Eisenman, Ian
Wagner, Till JW
et al.

Publication Date
2023-05-28

DOI
10.1029/2023gl103403

Peer reviewed

AGU
ADVANCING EARTH AND SPACE SCIENCE

Geophysical Research Letters®

Key Points:

- The seasonal cycle in zonal-mean surface air temperature is asymmetric
- The warming period tends to be shorter than 6 months in high latitudes and longer than 6 months in low latitudes
- The asymmetry can largely be explained by variations in top-of-atmosphere insolation, dictated by Earth's orbit

Supporting Information:

Supporting Information may be found in the online version of this article.

Correspondence to:

L. A. Roach,
l.roach@columbia.edu

Asymmetry in the Seasonal Cycle of Zonal-Mean Surface Air Temperature

Lettie A. Roach[1,2,3] , **Ian Eisenman**[4] , **Till J. W. Wagner**[5] , and **Aaron Donohoe**[6]

[1]NASA Goddard Institute for Space Studies, New York, NY, USA, [2]Center for Climate Systems Research, Columbia University, New York, NY, USA, [3]Cooperative Programs for the Advancement of Earth System Science, University Corporation for Atmospheric Research, Boulder, CO, USA, [4]Scripps Institution of Oceanography, University of California San Diego, La Jolla, CA, USA, [5]Atmospheric and Oceanic Sciences, University of Wisconsin-Madison, Madison, WI, USA, [6]Polar Science Center, Applied Physics Laboratory, University of Washington, Seattle, WA, USA

Abstract At most latitudes, the seasonal cycle of zonal-mean surface air temperature is notably asymmetric: the length of the warming season is not equal to the length of the cooling season. The asymmetry varies spatially, with the cooling season being ∼40 days shorter than the warming season in the subtropics and the warming season being ∼100 days shorter than the cooling season at the poles. Furthermore, the asymmetry differs between the Northern Hemisphere and the Southern Hemisphere. Here, we show that these observed features are broadly captured in a simple model for the evolution of temperature forced by realistic insolation. The model suggests that Earth's orbital eccentricity largely determines the hemispheric contrast, and obliquity broadly dictates the meridional structure. Clouds, atmospheric heat flux convergence, and time-invariant effective surface heat capacity have minimal impacts on seasonal asymmetry. This simple, first-order picture has been absent from previous discussions of the surface temperature seasonal cycle.

Plain Language Summary Away from the equator, most places on Earth experience a noticeable seasonal cycle in surface air temperature. The seasonal cycle of temperature governs many aspects of human and ecosystem behavior. Observations show that, at most latitudes, the length of the warming season is not equal to the length of the cooling season, that is, the seasonal cycle is *asymmetric*. For example, at 25°N, the average warming season is 35 days longer than the cooling season. Here, we look at how this asymmetry varies with distance from the equator. We find that the asymmetry can largely be explained as a result of variations in the amount of radiation from the sun that reaches Earth, which are determined by Earth's orbit.

1. Introduction

The seasonal cycle in surface air temperature is a fundamental feature of Earth's climate system, governing many aspects of human and ecological behavior. Qualitatively, it is understood that the seasonal cycle in temperature is driven by the seasonal cycle in insolation, and moderated primarily by the effective heat capacity of the surface, which damps the amplitude of the seasonal cycle over the ocean more than over the land. Seasonal variations in atmospheric circulation and spatial variations in radiative feedbacks also contribute to the seasonal evolution of temperature, and may provide an analog to the spatial pattern of warming expected in response to anthropogenic forcing (McKinnon et al., 2013). Quantitative understanding of the seasonal cycle in surface temperature and its changes under global warming has been developed through previous analyses that focus on the phase and amplitude of the annual harmonic (e.g., Donohoe & Battisti, 2013; Dwyer et al., 2012; Stine & Huybers, 2012; Stine et al., 2009).

However, as highlighted by Donohoe, Dawson et al. (2020), there are substantial departures in the surface air temperature from its annual harmonic that vary across the globe. These departures can be described using the difference in length between the periods of seasonal warming and cooling as a measure of asymmetry. Donohoe, Dawson et al. (2020) propose several candidate mechanisms that may explain asymmetry in various locations, including the atmospheric versus oceanic contrast in seasonal boundary layer depth in response to solar heating, the phase differences between surface insolation and top-of-atmosphere insolation due to clouds, and the impact of seasonally evolving atmospheric circulations such as the monsoon and stationary waves. Donohoe, Dawson et al. (2020) stress that their analysis is exploratory, and the authors find no single mechanism that adequately explains the broad-scale features of the asymmetry.
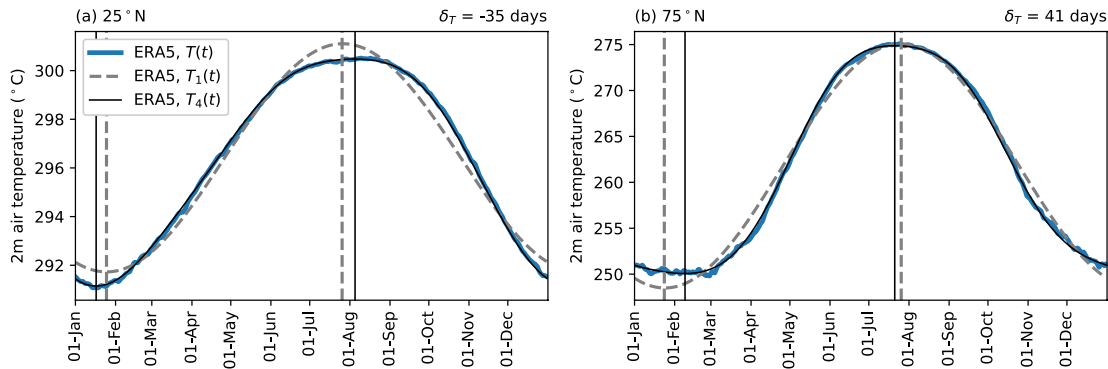
Figure 1. Example seasonal cycles of T2m at (a) 25° and (b) 75°N from ERA5, with data after spatial and temporal averaging shown in blue, the annual harmonic in gray dashed, and the Fourier fit with four harmonics in black. The times of maximum and minimum are indicated by vertical lines. The value of δ_T is marked in the upper right.

Here, we consider asymmetry in the seasonal cycle of zonal-mean surface air temperature, and in particular we focus on latitudinal variations in asymmetry (i.e., the meridional structure of the asymmetry). We show that the meridional structure of the asymmetry is consistent with idealized model results that describe the local thermodynamic response to the seasonal cycle in insolation, which features substantial departures from the annual harmonic in the high latitudes and subtropics. This model is cast as a simple ordinary differential equation (ODE) forced by realistic insolation; it is adopted from Roach et al. (2022) and applied here to a different question. The predicted asymmetry is found to be mostly insensitive to the inclusion of seasonally varying clouds, atmospheric circulation, and the specification of radiative feedbacks.

2. Methods

We use the daily 2-m air temperature (T2m) from the ERA5 reanalysis (Hersbach et al., 2020) and smooth it spatially by averaging the 0.25° data onto a coarser 2° grid. Leap years are linearly interpolated to 365 days. We then take the zonal mean and compute the climatology over the first four decades of the satellite era (1979–2018). Even after this spatial coarsening and temporal and spatial averaging, the seasonal cycle of T2m is visibly not smooth, and the computation of the timing of the maximum and the minimum of the seasonal cycle is sensitive to "noise" from internal variability. To further remove this noise, we fit a Fourier series with four harmonics to the zonal-mean climatological seasonal cycle of T2m at each latitude, θ. Specifically, we write

$$T_4(t,\theta) = \frac{1}{2}\xi_0(\theta) + \sum_{n=1}^{4} \xi_n(\theta)\cos[2\pi nt - \phi_n(\theta)],$$ (1)

where $\xi_n(\theta)$ and $\phi_n(\theta)$ are the Fourier coefficients (results are similar when using 2–10 harmonics, as shown in Figure S1 in Supporting Information S1). Figure 1 shows zonal-mean seasonal cycles at specific example latitudes from ERA5 alongside a Fourier series with one harmonic (T_1, which contains only the annual harmonic and is symmetric) and a Fourier series with four harmonics, T_4.

We then compute the days of maximum and minimum temperature from the Fourier fit with four harmonics, T_4 (vertical solid black lines in Figure 1). We define the length of the warming season as the duration from the minimum to the maximum of T_4. The length of the cooling season is similarly the duration from maximum to minimum, or equivalently 365 days minus the length of the warming season. As a measure of asymmetry, we define δ_T as the difference between the lengths of the warming and cooling seasons (as in Roach et al., 2022). Positive δ_T values represent a shorter warming season than cooling season, and negative values represent a shorter cooling season than warming season. For example, at 75°N, the date of minimum T_4 is delayed relative to its annual harmonic counterpart, whereas the date of maximum T_4 precedes maximum T_1 (see vertical black and gray-dashed lines in Figure 1b), with a warming season length of 162 days and a cooling season length of 203 days. This indicates a shorter warming season and positive δ_T, with $\delta_T = 41$ days.

Globally, results are similar using the JRA55 reanalysis (Japan Meteorological Agency, 2013) in place of ERA5, although there are some deviations over the Antarctic continent (Figure S2 in Supporting Information S1).
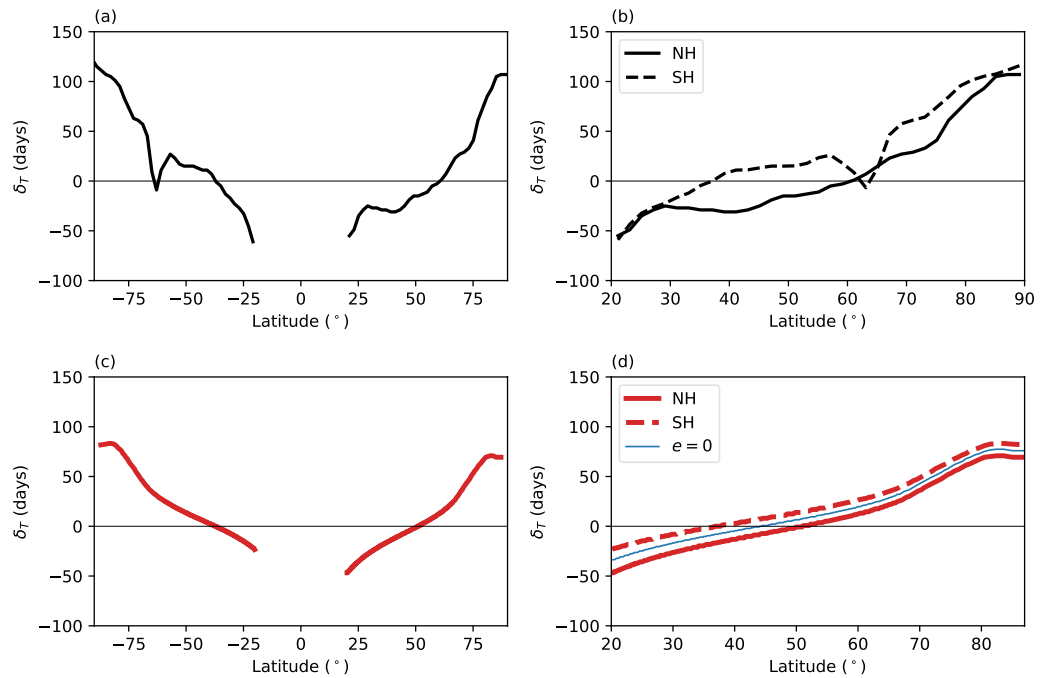
Figure 2. Meridional structure of asymmetry (δ_T). (a) Asymmetry computed from ERA5 output; (b) as in panel (a) but with values for the Southern Hemisphere plotted at their equivalent Northern latitudes. (c, d) As in panels (a, b) but for the solution to Equation 2, forced by present-day top-of-atmosphere (TOA) insolation. The thin blue line in panel (d) shows δ_T from the solution to Equation 2 with TOA insolation corresponding to zero orbital eccentricity.

3. Results

To investigate large-scale drivers of asymmetry in the seasonal cycle of T2m, we first consider the broad-scale structure in the zonal-mean seasonal cycle. Zonal variations in observed asymmetry are shown by Donohoe, Dawson, et al. (2020), who emphasize the land-ocean contrast in δ_T, which is readily apparent in the maps. Averaging T2m into the zonal mean reveals a striking meridional structure in observed δ_T (Figure 2a), which is the focus of the present study. Values of δ_T exceed 100 days near the poles, cross zero in the mid-latitudes, and reach −50 days in the tropics. Equatorward of 20°, we do not compute δ_T because there are typically two local maxima and minima in T2m each year. δ_T crosses zero ($\delta_T = 0$ days represents symmetry in the seasonal cycle of T2m) at 61° in the Northern Hemisphere and 37° in the Southern Hemisphere. There is a deviation from this overall pattern in the Southern Hemisphere, with δ_T crossing zero again at 64°S. The hemispheric differences are highlighted in Figure 2b by plotting values for the Southern Hemisphere at their equivalent Northern latitudes. Values in the two hemispheres are offset by around 20 days on average, with higher values in the Southern Hemisphere (Figure 2b).

We can gain understanding of the mechanisms controlling the meridional structure of δ_T using the framework of an idealized climate model. Roach et al. (2022) show that a substantial asymmetry in the seasonal cycle of temperature ($\delta_T \approx 1$ month) at high latitudes is obtained when solving a simple ODE in which seasonal variations in insolation are balanced locally by heating and radiative feedbacks. Hence we adopt Equation 7 from Roach et al. (2022):

$$c_w \frac{dT(t,\theta)}{dt} = a(\theta)S(t,\theta) - [A + BT(t,\theta)], \qquad (2)$$

where c_w is the heat capacity of the ocean mixed layer, chosen to approximate a 75 m mixed layer depth, T is the surface temperature departure from some reference value, and outgoing longwave radiation is approximated as $A + BT$ (Budyko, 1969; Koll & Cronin, 2018) with A and B constants. Top-of-atmosphere (TOA) insolation S is computed using present-day orbital parameters following Huybers and Eisenman (2006) and Rose (2018), and is scaled by planetary coalbedo a, where $a = a_0 - a_2 \sin^2\theta$ with a_0, and a_2 constants. Initial parameter values
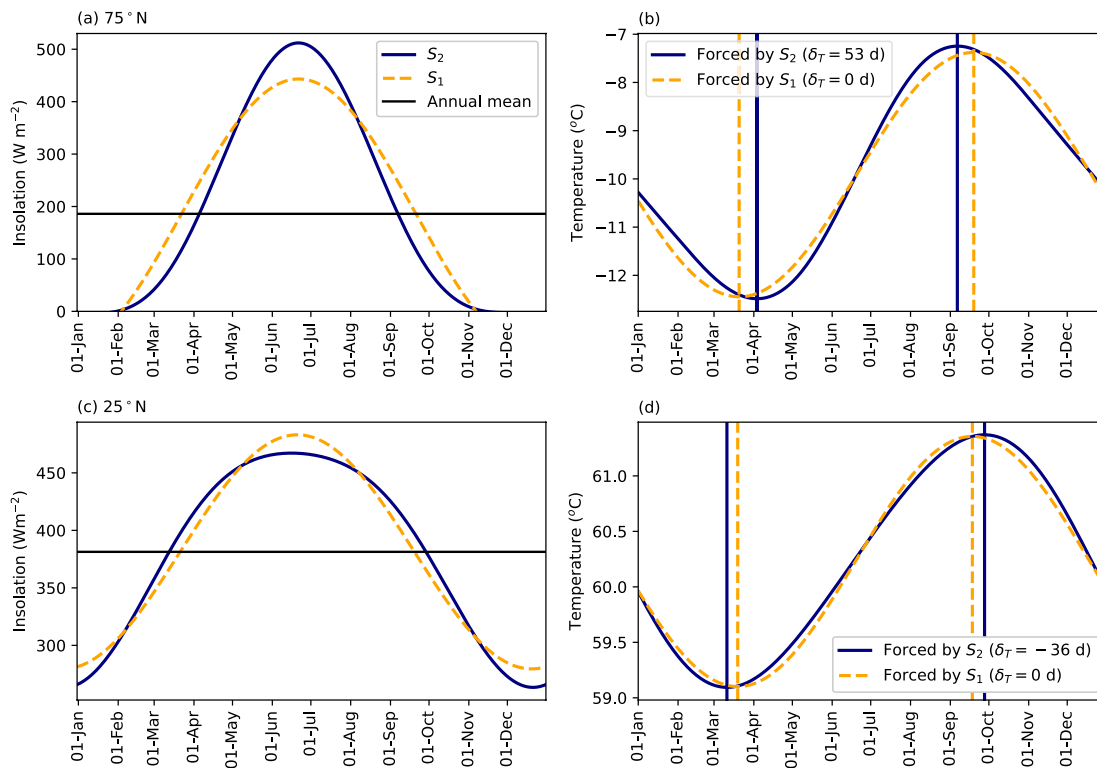
Figure 3. Left panels: Fourier series of the top-of-atmosphere insolation truncated at $N = 1$ and $N = 2$ at (a) 75° and (c) 25°N. Right panels: the solution $T(t)$ to Equation 2 when forced by the corresponding insolation as marked in the left panels, for (b) 75° and (d) 25°N.

are shown in Table S1 in Supporting Information S1. Note that asymmetry in temperature is always insensitive to changes in A. We solve Equation 2 numerically, using 100 simulation years, discretized with 1,000 timesteps per year and 800 gridboxes in one spatial dimension running from pole to pole (0.1° resolution at the equator to 2° at the poles). Importantly, the equation neglects many factors including seasonal variations in atmospheric heat transport and cloud albedo, and spatial variations in radiative feedbacks—we return to the impact of these neglected processes later.

The asymmetry in the seasonal cycle in temperature, δ_T, simulated using Equation 2 is shown in Figure 2c. This captures the broad-scale features shown in observations. In the simulations, δ_T decreases from 80 days near the poles to −50 days in the tropics. It crosses zero at 51° in the Northern Hemisphere and 37° in the Southern Hemisphere, similar to the observations. Values in the two hemispheres are offset by around 17 days on average, with higher values in the Southern Hemisphere (Figure 2d), as compared with 20 days in observations (Figure 2b). Thus, the simple ODE quantitatively reproduces two essential features of the observed spatial structure of δ_T: (a) more positive values in the Southern Hemisphere as compared to the same latitudes in the Northern Hemisphere and (b) positive values in the polar regions and negative values in the subtropics.

We first consider the hemispheric difference in δ_T. The eccentricity of Earth's orbit is key to the hemispheric difference in simulated temperature asymmetry. We re-compute TOA insolation using the code from Rose (2018) with eccentricity set to $e = 0$ rather than its present-day value of $e = 0.017$. In this case, solving Equation 2 yields identical values for both hemispheres (blue line in Figure 2d).

Second, we consider the meridional structure of δ_T, that is, the general pattern of increasing δ_T from negative values in the tropics to positive values near the poles, which is retained after setting eccentricity to zero. This general pattern results from the obliquity (or tilt) of Earth's rotation relative to the plane of its orbit, which causes the seasonal cycle to depart from its annual harmonic in ways that are qualitatively different at high and low latitudes (left panels of Figure 3). At high latitudes, the insolation minimum is prolonged and the insolation maximum is larger and more concentrated than its annual harmonic (Figure 3a). In contrast, at subtropical latitudes, the insolation minimum is more peaked while the insolation maximum is more prolonged than the corresponding annual harmonic (Figure 3c).

To understand how the departures in insolation from the annual harmonic impact δ_T, we further simplify Equation 2 by omitting radiative feedbacks, that is, setting $B = 0$. As discussed in Text S1 of Roach et al. (2022), the dominant balance in the ODE for annual forcing is between insolation and heating. Decomposing the insolation forcing as $S = \overline{S} + S'(t)$, where $\overline{S}$ is the annual mean and $S'(t) \equiv S - \overline{S}$ is the seasonally varying departure, and similarly for temperature, we obtain:

$$\frac{dT'(t,\theta)}{dt} = -\frac{T'(t,\theta)B}{c_w} + \frac{a(\theta)S'(t,\theta)}{c_w}. \tag{3}$$

In the regime where $\frac{dT'}{dt} \gg \frac{T'B}{c_w}$, this becomes

$$\frac{dT'(t,\theta)}{dt} \approx \frac{a(\theta)S'(t,\theta)}{c_w}, \tag{4}$$

which is Equation S4 in Roach et al. (2022). In this case, the temperature is in quadrature with the forcing. Therefore, having a narrow summer insolation peak with $S > \overline{S}$ and a wider winter insolation trough with $S < \overline{S}$, as occurs in high latitudes, leads to a brief summer warming period and a longer winter cooling period (Figure 3b). This is discussed equivalently for sea ice in Roach et al. (2022). Conversely, having a wide summer insolation peak with $S > \overline{S}$ and a narrow winter insolation trough with $S < \overline{S}$, as occurs in low latitudes, leads to a long summer warming period and a brief winter cooling period (Figure 3d).

The impact of obliquity on δ_T can be recovered when using only the first two harmonics of TOA insolation,

$$S_2(t,\theta) = \frac{1}{2}\xi_0(\theta) + \sum_{n=1}^{2} \xi_n(\theta)\cos[2\pi nt - \phi_n(\theta)], \tag{5}$$

to force Equation 2 (Figure S3 in Supporting Information S1). The solution for temperature in Equation 4 forced by two harmonics in insolation (Equation 5) is the superposition of two temperature harmonics in quadrature phase with the insolation harmonics,

$$T_2(t,\theta) \approx \frac{a(\theta)}{2\pi c_w} \sum_{n=1}^{2} n\xi_n(\theta)\sin[2\pi nt - \phi_n(\theta)]. \tag{6}$$

Thus, the temperature response to obliquity is essentially a consequence of the relative phasing of the annual and semi-annual components of insolation, which vary by latitude and sum to make the seasonal peaks and troughs of insolation broader or narrower than those of the annual harmonic alone.

While the broad-scale features of δ_T can be obtained considering only the remarkably simple Equation 2, we also consider some modifications to this expression. Simulated amplitudes for T can be brought into agreement with observations by tuning c_w for each latitude. Changes to c_w corresponding to ocean mixed layer depths between 10 and 200 m do not substantially alter δ_T (Figure S4 in Supporting Information S1). As c_w increases, the system remains in the regime where $\frac{dT'}{dt} \gg \frac{T'B}{c_w}$, so the temperature response remains in quadrature with the forcing. Minor differences in asymmetry arise when c_w tends toward the heat capacity of land, c_l (we use $c_l = 0.336$ W yr m^{-2} K^{-1} following North and Coakley (1979)), for example, over the fully land-covered latitudes of the Antarctic continent (Figure S5 in Supporting Information S1).

Equation 2 is conceptualized as a description of the surface energy balance with a parameterized radiative feedback to space forced by downwelling solar radiation at the surface. The modification of TOA insolation by co-albedo a in Equation 2 accounts for the reflection of insolation by clouds, but it assumes that cloud reflection is seasonally invariant. We assess how seasonally evolving cloud cover might impact δ_T by forcing Equation 2 instead with surface zonal-mean downwelling shortwave radiation from CERES (Doelling et al., 2013, 2016), that is, including the net shortwave effect of clouds instead of using TOA insolation. This has a relatively minor effect, although it amplifies asymmetry near the poles (Figure S6 in Supporting Information S1). Note that the higher values of δ_T here are somewhat closer to those seen in observations. We also modify Equation 2 to account in a simple way for atmospheric heat flux convergence, computed from ERA5 data by Donohoe, Armour, et al. (2020). The impact on δ_T is similar to or smaller in magnitude than switching from TOA to surface shortwave; note that it adds more meridional structure to the smooth curve that is obtained from Equation 2 alone (Figure S7 in Supporting Information S1).

As demonstrated by Donohoe, Dawson et al. (2020) (see also Figure S8a in Supporting Information S1), there are substantial zonal variations in asymmetry across the globe. To examine the role of zonal variations in cloud cover, we force Equation 2 with surface downwelling shortwave radiation from CERES across longitudes λ and solve for $T(\theta, \lambda)$. The impacts are minor in most regions, with the exception of the Indian subcontinent and the North Pacific (Figures S8b and S8f in Supporting Information S1). The seasonal cycle of the fraction of shortwave radiation absorbed by clouds over these two regions is nearly opposite. Over the Indian subcontinent, there are more clouds in the summer/early fall season due to summer monsoon activity, whereas in the North Pacific region, there are more clouds in the winter/spring season due to storm activity. Our simple model accounting for the impact of clouds cannot explain other zonally varying departures from the overall pattern expected based on insolation, including southeast of the South American continent and south of New Zealand.

4. Conclusions

The seasonal cycle of surface temperature has a large amplitude outside the tropics. Furthermore, the climatological seasonal evolution of temperature can serve as a test of our understanding of the underlying physics of the climate system, as it represents a well-observed response to a large change in solar forcing. The seasonal cycle is shaped by a variety of factors, including the tilt of the Earth's axis, Earth's orbital eccentricity, global atmospheric circulation patterns, and land surface characteristics. A number of previous studies have analyzed the seasonal cycle using the amplitude and phase of the annual harmonic, which is symmetric. However, at most latitudes, the seasonal cycle of temperature is strikingly asymmetric, deviating from symmetry by around −40 days in the subtropics and 100 days at the poles. Donohoe, Dawson et al. (2020) suggested a number of possible mechanisms that could contribute to this asymmetry, but nothing that could describe the broad-scale features.

Here, adopting the approach of Roach et al. (2022), we suggest that the broad meridional structure of asymmetry in the zonal-mean seasonal cycle of surface temperature results directly from variations in top-of-atmosphere insolation. The eccentricity of Earth's orbit generates the difference in asymmetry between the two hemispheres. The obliquity, or axial tilt, of the Earth generates much of the variation in asymmetry from the tropics to the poles, and it dictates the latitude where the seasonal cycle is symmetric. In the reanalysis products analyzed, values of asymmetry are on average 20 days higher in the Southern Hemisphere than the Northern Hemisphere (averaging over latitudes polewards of 20°). Using a simple idealized model of the evolution of surface temperature forced by realistic insolation, we reproduce both effects, with an average hemispheric difference of 17 days. Moreover, both effects can be captured using a simplified variant of the model forced by only two harmonics of the insolation.

We find that the asymmetry of the seasonal cycle of zonal-mean surface temperature arises primarily due to the direct thermodynamic response to insolation forcing. Our results suggest that clouds and atmospheric heat flux convergence do not play a substantial role in modulating the zonal-mean structure of asymmetry, although clouds impact temperature asymmetry in certain regions, specifically the North Pacific and the Indian subcontinent. Seasonal asymmetry may also be influenced by factors not considered here, including seasonal changes in surface effective heat capacity. The simple first-order picture presented here has been absent from previous discussions of the seasonal cycle of surface temperature.

Data Availability Statement

References

Budyko, M. I. (1969). The effect of solar radiation variations on the climate of the Earth. *Tellus*, *21*(5), 611–619. https://doi.org/10.3402/tellusa.v21i5.10109

Doelling, D. R., Loeb, N. G., Keyes, D. F., Nordeen, M. L., Morstad, D., Nguyen, C., et al. (2013). Geostationary enhanced temporal interpolation for CERES flux products. *Journal of Atmospheric and Oceanic Technology*, *30*(6), 1072–1090. https://doi.org/10.1175/JTECH-D-12-00136.1

Doelling, D. R., Sun, M., Nguyen, L. T., Nordeen, M. L., Haney, C. O., Keyes, D. F., & Mlynczak, P. E. (2016). Advances in geostationary-derived longwave fluxes for the CERES synoptic (SYN1deg) product. *Journal of Atmospheric and Oceanic Technology*, *33*(3), 503–521. https://doi.org/10.1175/JTECH-D-15-0147.1

Donohoe, A., Armour, K. C., Roe, G. H., Battisti, D. S., & Hahn, L. (2020). The partitioning of meridional heat transport from the Last Glacial Maximum to CO_2 quadrupling in coupled climate models. *Journal of Climate*, *33*(10), 4141–4165. https://doi.org/10.1175/JCLI-D-19-0797.1

Donohoe, A., & Battisti, D. S. (2013). The seasonal cycle of atmospheric heating and temperature. *Journal of Climate*, *26*(14), 4962–4980. https://doi.org/10.1175/JCLI-D-12-00713.1

Donohoe, A., Dawson, E., McMurdie, L., Battisti, D. S., & Rhines, A. (2020). Seasonal asymmetries in the lag between insolation and surface temperature. *Journal of Climate*, *33*(10), 3921–3945. https://doi.org/10.1175/jcli-d-19-0329.1

Dwyer, J. G., Biasutti, M., & Sobel, A. H. (2012). Projected changes in the seasonal cycle of surface temperature. *Journal of Climate*, *25*(18), 6359–6374. https://doi.org/10.1175/JCLI-D-11-00741.1

Hersbach, H., Bell, B., Berrisford, P., Hirahara, S., Horányi, A., Muñoz-Sabater, J., et al. (2020). The ERA5 global reanalysis. *Quarterly Journal of the Royal Meteorological Society*, *146*(730), 1999–2049. https://doi.org/10.1002/qj.3803

Huybers, P., & Eisenman, I. (2006). *Integrated summer insolation calculations*. IGBP PAGES/World Data Center for Paleoclimatology. (Place: NOAA/NCDC Paleoclimatology Program.

Japan Meteorological Agency. (2013). JRA-55: Japanese 55-year reanalysis, daily 3-hourly and 6-hourly data. https://doi.org/10.5065/D6HH6H41

Koll, D. D. B., & Cronin, T. W. (2018). Earth's outgoing longwave radiation linear due to H_2O greenhouse effect. *Proceedings of the National Academy of Sciences of the United States of America*, *115*(41), 10293–10298. https://doi.org/10.1073/pnas.1809868115

McKinnon, K. A., Stine, A. R., & Huybers, P. (2013). The spatial structure of the annual cycle in surface temperature: Amplitude, phase, and Lagrangian history. *Journal of Climate*, *26*(20), 7852–7862. https://doi.org/10.1175/JCLI-D-13-00021.1

North, G. R., & Coakley, J. A. (1979). Differences between seasonal and mean annual energy balance model calculations of climate and climate sensitivity. *Journal of the Atmospheric Sciences*, *36*(7), 1189–1204. https://doi.org/10.1175/1520-0469(1979)036<1189:DBSAMA>2.0.CO;2

Roach, L. A., Eisenman, I., Wagner, T. J. W., Blanchard-Wrigglesworth, E., & Bitz, C. M. (2022). Asymmetry in the seasonal cycle of Antarctic sea ice driven by insolation. *Nature Geoscience*, *15*(4), 277–281. https://doi.org/10.1038/s41561-022-00913-6

Rose, B. E. J. (2018). CLIMLAB: A Python toolkit for interactive, process-oriented climate modeling. *Journal of Open Source Software*, *3*(24), 659. https://doi.org/10.21105/joss.00659

Stine, A. R., & Huybers, P. (2012). Changes in the seasonal cycle of temperature and atmospheric circulation. *Journal of Climate*, *25*(21), 7362–7380. https://doi.org/10.1175/JCLI-D-11-00470.1

Stine, A. R., Huybers, P., & Fung, I. Y. (2009). Changes in the phase of the annual cycle of surface temperature. *Nature*, *457*(7228), 435–440. https://doi.org/10.1038/nature07675